

Plasma-Enhanced Chemical Vapor Deposition of Organosilicon Materials: A Comparison of Hexamethyldisilane and Tetramethylsilane Precursors

J. L. C. Fonseca, S. Tasker, D. C. Apperley,[†] and J. P. S. Badyal*

Department of Chemistry, Science Laboratories, University of Durham, Durham DH1 3LE, England

Received February 22, 1995; Revised Manuscript Received October 30, 1995[§]

ABSTRACT: Plasma polymerization of hexamethyldisilane ($[\text{CH}_3]_3\text{SiSi}[\text{CH}_3]_3$) and tetramethylsilane ($[\text{CH}_3]_4\text{Si}$) has been investigated by XPS, FTIR, solid state NMR, and plasma emission diagnostics. Thin carbosilane films and powders can be deposited by this method. Hexamethyldisilane is found to undergo glow discharge polymerization much more readily than tetramethylsilane; this has been attributed to the chromophoric $\text{Si}-\text{Si}$ bond contained in the former precursor.

Introduction

Plasma-polymerized organosilicon layers are promising materials for use in biocompatible coatings,¹ integrated optical circuitry,^{2,3} and semiconductor device fabrication,⁴ as precursors for the synthesis of silicon carbide,⁵ as moisture barrier coatings,⁶ and as adhesion promoters between glass fibers and polymer matrices.⁷ Tetramethylsilane ($[\text{CH}_3]_4\text{Si}$),^{8,9} phenylsilane ($[\text{C}_6\text{H}_5]\text{SiH}_3$),¹⁰ trimethylvinylsilane ($[\text{CH}_3]_3\text{Si}[\text{CHCH}_2]$),¹¹ and hexamethyldisilane ($[\text{CH}_3]_3\text{Si}-\text{Si}[\text{CH}_3]_3$)¹² are among some of the carbosilane monomers previously studied. Silylmethyl groups, $[\text{CH}_3]_x\text{Si}$ ($x = 1-3$), and weak Si-Si linkages are understood to play a key role during the plasma polymerization of organosilanes.¹³

In this article, a comparison is made between the nonequilibrium glow discharge polymerization of tetramethylsilane ($[\text{CH}_3]_4\text{Si}$) and hexamethyldisilane ($[\text{CH}_3]_3\text{Si}-\text{Si}[\text{CH}_3]_3$). These precursors are structurally identical apart from the weak Si-Si linkage contained in the latter molecule. Coatings and powders have been synthesized from each of these monomers and characterized by XPS, FTIR, NMR, and XRD. UV emission spectroscopy measurements have been made on the organosilane glow discharges. A mechanistic insight into the polymerization and structural aspects of these carbosilicon materials is presented.

Experimental Section

Tetramethylsilane (TMS, 99.9% Aldrich Chemicals) and hexamethyldisilane (HMDS, 98% Aldrich Chemicals) were further purified by multiple freeze-pump-thaw cycles. These reagents were found to have a sufficiently high vapor pressure at room temperature and therefore did not require any external warming. Two types of substrate were used: low-density polyethylene films (LDPE, Metal Box) and glass slides. Both of these were washed with isopropyl alcohol, and dried prior to use.

Glow discharge experiments were carried out in a cylindrical glass reactor (4.5 cm diameter, 490 cm³ volume) enclosed in a Faraday cage.¹⁴ It was fitted with a monomer inlet, a Pirani pressure gauge, and a 47 L min⁻¹ two-stage rotary pump attached to a liquid nitrogen cold trap. A 13.56 MHz radio frequency (RF) source was inductively coupled to the reactor via a matching network and a copper coil (4 mm diameter, 9

turns) spanning 11.0–18.5 cm from the monomer inlet. Average excitation powers lower than 5 W could be sustained by pulsing the glow discharge. All joints were grease-free. A fixed substrate position of 6.5 cm from the reactor inlet was used for the experiments concerned with investigating the effects of W/F_M upon plasma polymer growth. In the case of bulk material studies, powdered deposit was collected from all parts of the reaction vessel. Calculation of monomer and leak mass flow rates assumed ideal gas behavior.¹⁵

A typical experimental run consisted of first scrubbing the reactor with detergent, rinsing with isopropyl alcohol, and drying, which was then followed by a high-power (50 W) air plasma treatment lasting 60 min. This last step was carried out in the presence of glass substrates, but in the absence of polyethylene film, since oxygen glow discharges are renowned for their ability to oxidize polymer surfaces.¹⁶ Next, the reactor was pumped down to its base pressure of 2×10^{-2} Torr and a leak rate of better than 2.6×10^{-10} kg/s. Subsequently, the monomer was introduced into the reaction chamber at 1×10^{-1} Torr pressure and mass flow rates (F_M) of 3.6×10^{-8} and 4.3×10^{-8} kg/s for TMS and HMDS, respectively (i.e. at least 99.3% of F_M is the organosilane precursor). Following 5 min of purging, the glow discharge was ignited. Upon completion of deposition, the RF source was switched off, the monomer reservoir closed, and the reactor evacuated back to its original base pressure for at least 5 min. Finally, the system was let up to atmosphere, and the appropriate analytical measurement undertaken.

X-ray photoelectron spectra were acquired on a Kratos ES200 surface analysis instrument operating in the fixed retarding ratio (22:1) analyzer mode. Magnesium K α X-rays were used as the photoexcitation source with an electron takeoff angle of 30° from the surface normal. Instrument performance was calibrated with respect to the gold 4f_{7/2} level at 83.8 eV with a full-width-at-half-maximum (FWHM) of 1.2 eV. No radiation damage was observed during the typical time scale involved in these experiments. An IBM PC computer was used for data accumulation and component peak analysis (assuming linear background subtraction and Gaussian fits with fixed FWHM). All binding energies are referenced to the hydrocarbon ($-\text{C}_2\text{H}_5-$) component at 285.0 eV.¹⁷ Instrumentally determined sensitivity factors for unit stoichiometry were taken as C(1s):O(1s):Si(2p) equals 1.00:0.55:1.05.

Infrared absorbance spectra of powdered material and coated polyethylene film were collected on a FTIR Mattson Polaris instrument. Plasma polymer powder was mixed with dried KBr, then pressed into a disk, and characterized by the transmission method. Treated polyethylene film was mounted onto a variable angle attenuated total reflection (ATR) cell fitted with a KRS-5 crystal. An incident beam angle of 45° was used, which resulted in 14 internal reflections.¹⁸ Typically, 100 scans were acquired at a resolution of 4 cm⁻¹.

Solid-state NMR spectra were taken on a Varian VXR-300 spectrometer equipped with a Doty Scientific magic-angle-

* To whom correspondence should be addressed.

[†] Industrial Research Laboratories, University of Durham, Durham DH1 3LE, England.

[§] Abstract published in *Advance ACS Abstracts*, February 1, 1996.

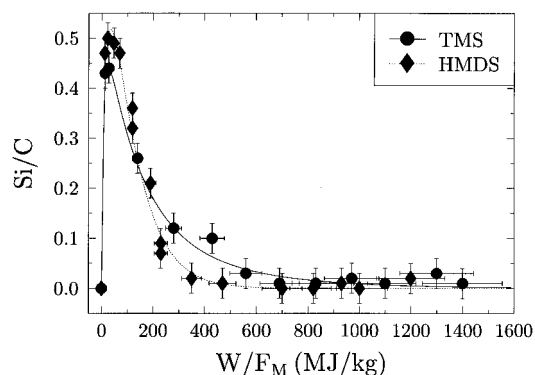


Figure 1. Si/C ratios as a function of glow discharge power: (a) TMS; (b) HMDS. (6.5 cm from monomer inlet, 10 min deposition).

spinning (MAS) probe. ^{29}Si and ^{13}C NMR signals were recorded at 59.6 and 75.4 MHz, respectively. In both cases, tetramethylsilane (TMS) was used as the chemical shift reference. Cross-polarization (CP) spectra were obtained with a 3 ms contact time and a 2 s relaxation delay. Additional ^{29}Si spectra were acquired following 90° pulses (of 4 μs) having relaxation delays of 5 and 60 s. In all cases, sample spin rates were maintained at approximately 4 kHz.

A home-built UV emission spectrometer based upon a Czerny-Turner type monochromator was used for plasma glow analysis. A computer was used to rotate the grating via a stepping motor and also to accumulate the counts from the photomultiplier tube detector. This instrument could scan continuously from 180 to 500 nm at 0.5 nm resolution.

Nitrogen adsorption isotherms were determined for each sample using a PMI Brookhaven Sorption apparatus. The Brunauer, Emmett, and Teller (BET) method for specific surface area determination was employed. Elemental microanalysis was done on a Carlo Erba elemental analyzer (model 1106). A Philips X-ray diffractometer (model PW1009/80) fitted with a Cu $K\alpha$ ($\lambda = 1.5443 \text{ \AA}$) tube and a Debye-Scherrer camera was used to determine whether the collected plasma powder possessed any crystalline character.

Results

Short deposition times resulted in a uniform coating; however longer times (6 h) produced a substantial amount of noncrystalline brown powder within the glow region. The HMDS material (surface area = $11.92 \pm 0.22 \text{ m}^2 \text{ g}^{-1}$) changed to a yellow color on standing in air, whereas its TMS counterpart (surface area = $17.10 \pm 0.98 \text{ m}^2 \text{ g}^{-1}$) retained its brown appearance. Elemental microanalysis of the collected plasma deposits (at maximum deposition rates, see below) yielded H/C ratios of 1.9 and 2.3 for TMS and HMDS, respectively, whereas the H/C ratio for both monomers is 3.0.

X-ray Photoelectron Spectroscopy. The Si/C ratios of plasma-polymerized organosilicon coatings deposited onto a polyethylene substrate were found to drop with increasing W/F_M , leading to hydrocarbon-rich films, Figure 1; this fall in Si/C ratio is much more pronounced for HMDS. Also, a greater silicon content was found in the HMDS product at very low excitation energies. The Si(2p) peak is centered on $100.7 \pm 0.1 \text{ eV}$ for the TMS plasma powder, whereas it is shifted to $101.2 \pm 0.1 \text{ eV}$ in the case of HMDS. Angle-resolved XPS studies of both organosilicon deposits revealed a small amount of surface oxygen at increased glancing angles (less than 4%), this probably originated from the reaction of trapped free radicals in the plasma polymer reacting with the atmosphere during sample transfer to the XPS spectrometer.

FTIR Spectroscopy. Characteristic infrared absorption bands for the TMS molecule can be assigned

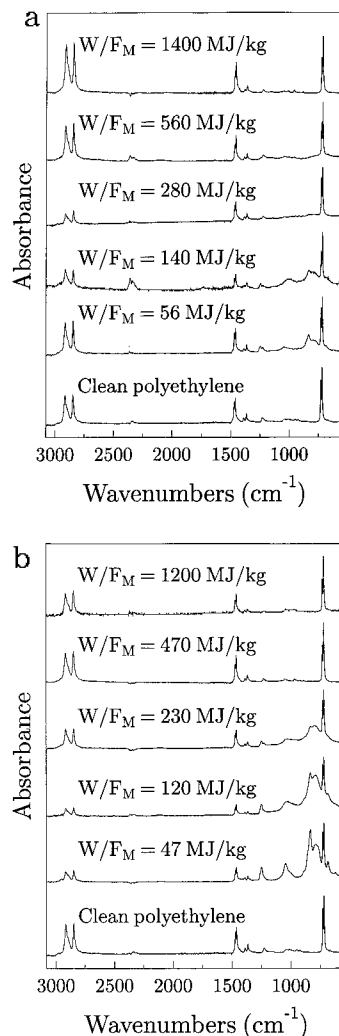


Figure 2. ATR-FTIR spectra of plasma-polymerized organosilane onto polyethylene as a function of W/F_M : (a) TMS; (b) HMDS. (6.5 cm from monomer inlet, 10 min deposition).

as follows:¹⁹ 2955 cm^{-1} (C–H asymmetrical stretching in CH_3), 2891 cm^{-1} (C–H symmetrical stretching in CH_3), 1248 cm^{-1} (CH_3 symmetric bending in $\text{Si}[\text{CH}_3]_n$), 864 cm^{-1} (CH_3 rocking in $\text{Si}[\text{CH}_3]_n$), and 694 cm^{-1} (Si–C stretching). The hexamethyldisilane precursor gives rise to the following infrared absorption bands:¹⁹ 2951 cm^{-1} (C–H asymmetrical stretching in CH_3), 2893 cm^{-1} (C–H symmetrical stretching in CH_3), 1246 cm^{-1} (CH_3 symmetric bending in $\text{Si}[\text{CH}_3]_n$), 835 cm^{-1} (CH_3 rocking in $\text{Si}[\text{CH}_3]_n$), and 721 , 690 , and 607 cm^{-1} (Si–C stretching). The Si–Si stretch in HMDS is infrared-inactive.

ATR-FTIR studies using a polyethylene substrate were used to determine the optimum conditions for maximum deposition rate of organosilicon material. The greatest attenuation of the characteristic polyethylene bands was taken as corresponding to the thickest plasma polymer layer. By using this method, it was deduced that carbosilane polymerization occurs most rapidly at $W/F_M = 280 \text{ MJ/kg}$ for TMS and $W/F_M = 120 \text{ MJ/kg}$ for HMDS, Figure 2.

FTIR transmission spectra of powdered material obtained from plasma polymerization of TMS and HMDS (at maximum deposition rates) are compared in Figure 3. Typically, CH_3 stretching bands tend to occur at 2962 cm^{-1} (C–H asymmetrical stretching) and 2872 cm^{-1} (C–H symmetrical stretching).²⁰ Methylene groups (CH_2) in aliphatic and nonstrained cyclic hydrocarbons exhibit C–H asymmetrical and symmetrical stretches

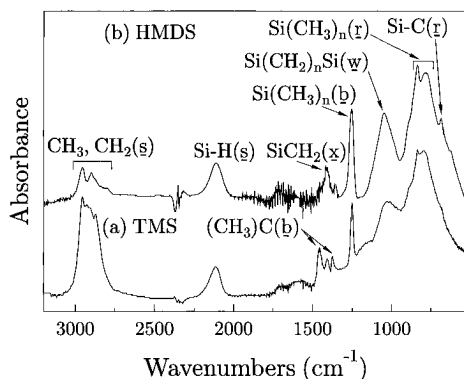


Figure 3. Transmission FTIR spectra of powdered glow discharge deposit: (a) TMS ($W/F_M = 280$ MJ/kg); (b) HMDS ($W/F_M = 120$ MJ/kg). Key: Stretching (s), rocking (r), bending (b), scissoring (x), and wagging (w).

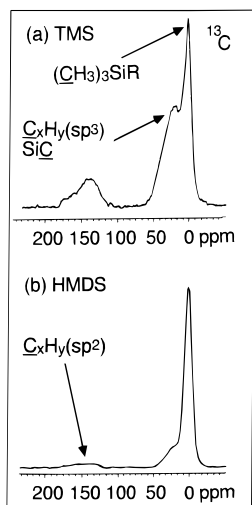


Figure 4. ^{13}C NMR spectra of powdered glow discharge deposit: (a) TMS ($W/F_M = 280$ MJ/kg); (b) HMDS ($W/F_M = 120$ MJ/kg).

at 2926 and 2853 cm^{-1} , respectively (the exact position can vary by up to ± 10 cm^{-1}). Any type of strain can cause the aforementioned stretching frequencies to increase.²⁰ Therefore the 2951 and 2895 cm^{-1} bands seen in the FTIR spectra of the freshly deposited powders arise from the overlap between CH_3 and CH_2 stretching frequencies. $\text{CH}_3\text{-C}$ linkages can also be identified by peaks at 1460 cm^{-1} (methyl asymmetric bending in $\text{CH}_3\text{-C}$) and 1375 cm^{-1} (methyl symmetric bending in $\text{CH}_3\text{-C}$). Silicon-related infrared absorptions are assignable as follows:^{9,11,19,21-25} 2110 cm^{-1} (Si-H stretching), 1408 cm^{-1} (CH_2 symmetrical scissoring in Si-CH_2), 1250 cm^{-1} (CH_3 symmetric bending in $\text{Si}[\text{CH}_3]_n$), 1026 cm^{-1} (Si-O-Si and/or Si-O-C asymmetric stretching and/or CH_2 wagging in $\text{Si-}[\text{CH}_2]_n\text{-Si}$), 833 cm^{-1} (CH_3 rocking in $\text{Si}[\text{CH}_3]_n$, $n = 2, 3$), 791 cm^{-1} (CH_3 rocking in $\text{Si}[\text{CH}_3]_n$, $n = 1, 2$), and 685 cm^{-1} (Si-C stretching). Clearly, HMDS gives rise to a silicon-rich plasma polymer, consisting of mainly Si-CH_2 , $\text{Si-}[\text{CH}_2]_n\text{-Si}$, and $\text{Si}[\text{CH}_3]_n$ moieties, whereas the TMS product contains a greater organic content.

Solid State NMR. ^{13}C and ^{29}Si NMR spectra of freshly deposited TMS and HMDS plasma polymers are shown in Figures 4 and 5, respectively. All NMR measurements have been referenced to tetramethylsilane monomer. Characteristic features observed in these spectra have been assigned in accordance with data published elsewhere.^{22,26-29} The most intense ^{13}C and ^{29}Si NMR signals are located at around 0 ppm.

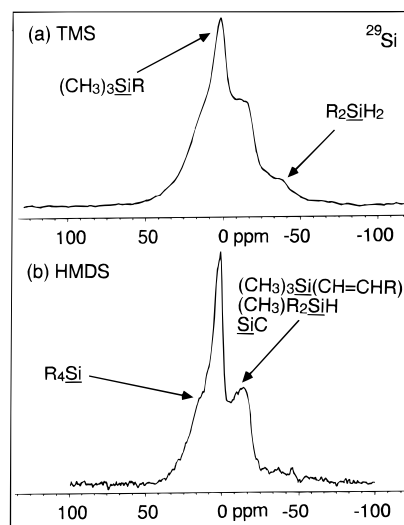


Figure 5. ^{29}Si NMR spectra of powdered glow discharge deposit: (a) TMS ($W/F_M = 280$ MJ/kg); (b) HMDS ($W/F_M = 120$ MJ/kg).

Therefore the major chemical environment present in these plasma deposits is very similar to that found in the TMS reference compound (i.e. $\text{Si}[\text{CH}_3]_n$).

The shoulder at approximately 20–50 ppm in the ^{13}C NMR spectra is characteristic of either sp^3 carbon atoms located within a hydrocarbon chain, or silicon carbide species;²⁶ clearly, this feature is much more intense for the TMS product, which would be consistent with it having a greater organic content. Unsaturated centers are evident in the 120–180 ppm range (the occurrence of carbonyl groups in the freshly deposited materials can be ruled out, since none were detected by infrared analysis); in fact there appears to be a higher proportion of unsaturated carbon linkages in the TMS plasma polymer.

The ^{29}Si NMR spectra for both materials comprise a strong signal centered at 1 ppm which is characteristic of $-\text{Si}[\text{CH}_3]_3$ fixed to hydrocarbon chain ends, the slight shoulder on this peak at 6 ppm is most likely to originate from silicon centers fixed to hydrocarbon chains, of the type R_4Si , where not more than one R chain is a methyl group. The peak at approximately -11 to -14 ppm can be attributed to one or more of the following: silicon centers with unsaturated carbon centers attached to the β position from the $[\text{CH}_3]_3\text{Si}$ group of the type $[\text{CH}_3]_3\text{Si}[\text{CH=CHR}]$ where $\text{R} = \text{H}$, CH_3 , or $\text{Si}[\text{CH}_3]_3$ or $[\text{CH}_3]\text{R}_2\text{SiH}$, provided R has an alkyl chain containing at least two $[-\text{CH}_2-]$ linkages, or perhaps silicon carbide type species. The weak feature at -35.0 ppm is most likely to be some kind of $\text{R}^1\text{R}^2\text{-SiH}_2$ linkage. The ^{29}Si NMR results are consistent with ^{13}C NMR experiments: TMS plasma polymer has a higher organic content and contains a greater number of unsaturated carbon centers.

Emission Spectroscopy. Most of the lines in the carbosilane emission spectra³⁰ originate from electronic transitions within the hydrogen molecule (230–310 nm vibrational-rotational continuum, 363.3, 367.3, 379.9, 385.8, 387.1, 388.6, 406.1, 406.6, 406.9, 417.4, 420.1, 422.0, 433.8, 449.0, 449.6, 455.4, 458.0, 461.5, 463.2, and 461.5 nm)^{31,32} and hydrogen atom Balmer lines (486.1 and 434.1 nm).³³ Other strong lines are due to the $\text{C}^3\Pi_u \rightarrow \text{B}^3\Pi_g$ transition for a nitrogen molecule:³⁴ 315.9 nm ($v' = 1, v'' = 0$), 337.1 nm (0, 0), and 357.7 nm (0, 1). It is important to take into consideration that these nitrogen lines are weaker by an approximate factor of

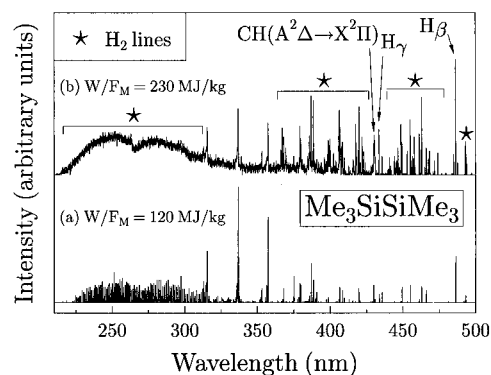


Figure 6. Emission spectra of HMDS glow discharges: (a) $W/F_M = 120$ MJ/kg; (b) $W/F_M = 230$ MJ/kg.

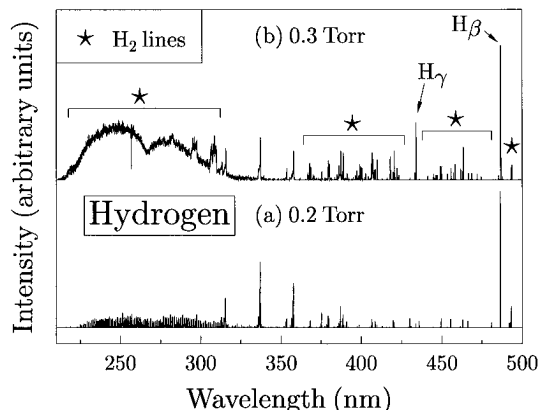


Figure 7. Emission spectra of pure molecular hydrogen glow discharges (10 W): (a) 0.2 Torr; (b) 0.3 Torr.

2000 compared to their intensity in a pure nitrogen plasma, and therefore the actual amount of molecular nitrogen in the reactor during plasma polymerization must be less than 0.05%. A very weak emission line is discernible at 493.6 nm, which is probably due to the $A^2\Pi \rightarrow X^2\Sigma$ transition for a CN radical^{35,36} (CN radicals are widely reported to be present as impurity species in hydrocarbon glow discharges³⁷). Finally, a band corresponding to the $A^2\Delta \rightarrow X^2\Pi$ transition for a CH radical was observed at 431.4 nm.^{38,39}

At high deposition rates ($W/F_M = 120$ MJ/kg), the HMDS glow discharge does not exhibit much emission from atomic or molecular hydrogen, Figure 6. On raising the RF power ($W/F_M = 230$ MJ/kg), the molecular hydrogen features undergo a greater increase in signal strength relative to the atomic hydrogen lines. This observation can be explained by referring to the emission spectra from pure hydrogen plasmas at different inlet gas pressures, Figure 7: the atomic and molecular hydrogen intensities increase at higher hydrogen pressures. Therefore it can be concluded that more atomic and molecular hydrogen formation occurs in the case of the $W/F_M = 230$ MJ/kg HMDS glow discharge.

For the TMS glow discharges, some gaps are clearly evident within the 225–350 nm molecular hydrogen emission continuum: at 238–240, 243–247, 255–258, 290–293, and 298–313 nm, Figure 8. The most likely explanation for these absences is that the TMS plasma medium contains unsaturated species which are strongly absorbing at these wavelengths. For instance, acetylene absorbs in the 220–240 nm range;^{40,41} another possibility may be the propargyl radical ($\text{CH}_2\text{—C=CH}$) which exhibits diffuse bands at 290–345 nm (strongest being at 332, 321.7, and 311.9 nm⁴²) or perhaps diacetylene

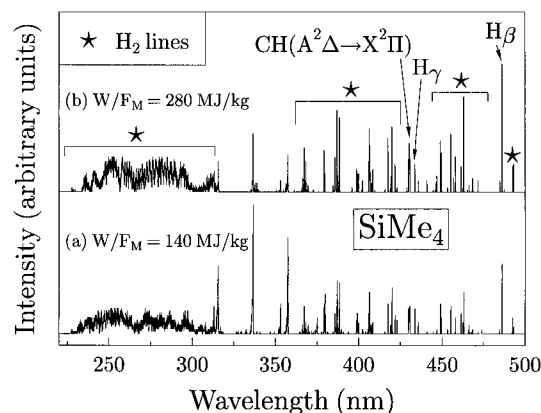
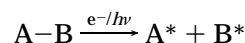


Figure 8. Emission spectra of TMS glow discharges: (a) $W/F_M = 140$ MJ/kg; (b) $W/F_M = 280$ MJ/kg.

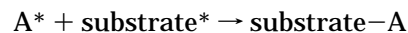
which has 700 narrow bands between 297 and 206.8 nm.⁴³

Discussion

Plasma polymerization processes are widely regarded as being highly complex in nature. Typically, they involve dissociation, generation, and recombination of polymerizable species within either the partially ionized gas itself and/or at the substrate surface.^{44–46} Such reactions are perpetuated by electron impact and ultraviolet radiation. In simple terms



where A and B may be individual atoms or molecular fragments which generate activated species A^* and B^* (ions and radicals). These intermediates can subsequently recombine to form new chemical species or impinge onto a substrate (which may also have been activated by the plasma), leading to the formation and growth of a plasma-polymerized layer:

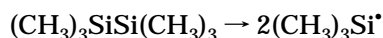


This description is appropriate for short plasma polymerization periods and low deposition rates; however powdered material can be generated by using either longer times (polyethylene films coated with thick carbosilane plasma polymer layers tend to curl up due to large internal stresses^{47,48}) or higher deposition rates.⁴⁹

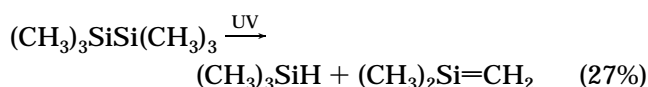
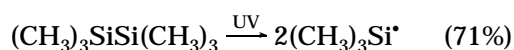
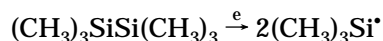
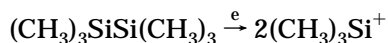
XPS, FTIR, and solid state NMR measurements show that $[\text{CH}_3]_n\text{Si}$ linkages are the major functionalities for both TMS and HMDS plasma polymers. It can also be concluded from XPS and FTIR that the TMS product contains a higher proportion of organic species. The brown appearance of freshly deposited polymerization products is indicative of unsaturated centers. The fact that HMDS plasma polymer discolors with time, whereas its TMS counterpart remains brown and possesses a smaller H/C elemental ratio, is consistent with the latter material containing a higher proportion of sp^2 carbon centers. The lower Si(2p) XPS binding energy value for the TMS plasma polymer can be explained in terms of this material being effectively electron-rich in view of its unsaturated character. Solid state NMR experiments are in agreement with the aforementioned description, since the ^{13}C sp^2 and the ^{29}Si $[\text{CH}_3]_3\text{Si—}[\text{CH=CHR}]$ environments are of greater intensity for the TMS experiments. Emission spectroscopy of the TMS glow discharge provides further evidence for the

generation of chromophoric/unsaturated moieties during plasma polymerization.

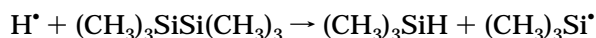
Estimated bond energy values are as follows:^{50–52} Si–Si (196 kJmol^{–1}), Si–C (292 kJmol^{–1}), and C–H (416 kJmol^{–1}). Incorporation of [CH₃]_nSi species into the plasma polymers (as detected by NMR, FTIR, and mass spectrometry²⁵) is consistent with the rupture of [CH₃]₃Si–Si[CH₃]₃, [CH₃]₃Si–CH₃, and [CH₃]₃SiCH₂–H bonds. The only structural difference between the TMS and HMDS precursors is the Si–Si linkage present in the latter molecule. The greater reactivity of the HMDS monomer must therefore arise from its chromophoric Si–Si linkage. HMDS is reported to undergo homolytic fission during thermal decomposition:⁵⁰



Electron–molecule⁵³ and photon–molecule⁵⁴ reactions are likely to be two of the key processes responsible for ionization and dissociation within the HMDS glow discharge:



Intermediate silene species can readily propagate chain growth due to their diradical nature.⁵⁵ Also, the following reaction is likely to be important,⁵⁶ since emission spectroscopy has shown that the HMDS glow discharge contains a significant amount of atomic hydrogen:



Such trimethylsilicon species may undergo reaction with free radical centers at the substrate surface,⁵⁷ whereas for TMS, plasma polymerization will only occur after a number of fragmentation and rearrangement steps (hence the prerequisite for higher glow discharge energies in this case). Extensive breakdown of the incoming precursor molecule, and greater sputtering of the growing plasma polymer layer are more likely to generate unsaturated linkages.

Conclusions

Plasma polymerization of the structurally related tetramethylsilane (TMS) and hexamethyldisilane (HMDS) molecules results in extended organosilicon networks. TMS plasma polymer contains a higher proportion of organic entities and possesses a significant degree of unsaturation, whereas the HMDS-derived material has a greater number of [CH₃]_nSi linkages. These differences in plasma product can be related to the mode of precursor decomposition within the nonisothermal glow discharge. TMS has to undergo a relatively greater extent of fragmentation in order to generate solid-forming moieties. In contrast to this, HMDS is capable of easily decomposing under milder conditions to form polymerizable species due to its inherently weak [CH₃]₃Si–Si[CH₃]₃ linkage.

Acknowledgment. J.L.C.F. thanks Brazil's Conselho Nacional de Desenvolvimento Científico e Tecnológico for financial support during the course of this work.

References and Notes

- (1) Yasuda, H.; Bumgarner, M. O.; Marsch, H. C.; Morosoff, N. *J. Polym. Sci., Polym. Chem. Ed.* **1976**, *14*, 195.
- (2) Tien, P. K.; Smolinsky, G.; Martin, R. *J. Appl. Opt.* **1972**, *11*, 637.
- (3) Tyczkowski, J.; Odrobina, E.; Kazimierski, P.; Bassler, H.; Kisiel, A.; Zema, N. *Thin Solid Films* **1992**, *209*, 250.
- (4) Larkin, D. J.; Interrane, L. V. *Chem. Mater.* **1992**, *4*, 22.
- (5) Konotek, O.; Löffler, F. *Mater. Sci. Eng.* **1991**, *A140*, 655.
- (6) Sacher, E.; Klemberg-Sapieha, J. E.; Schreiber, H. P.; Wertheimer, M. R. *J. Appl. Polym. Sci., Appl. Polym. Symp.* **1984**, *38*, 149.
- (7) Krishnamurthy, V.; Kamel, I. L.; Wei, Y. *J. Appl. Polym. Sci.* **1989**, *38*, 605.
- (8) Nguyen, V. S.; Underhill, J.; Fridmann, S.; Pan, P. *J. Electrochem. Soc.* **1985**, *132*, 1925.
- (9) Park, S. Y.; Kim, N.; Hong, S. I.; Sasabe, H. *Polym. J.* **1990**, *22*, 242.
- (10) Laoharojanaphand, P.; Lin, T. J.; Stoffer, J. O. *J. Appl. Polym. Sci.* **1990**, *40*, 369.
- (11) Kruse, A.; Hennecke, M.; Baalman, A.; Schlett, V.; Stuke, H. *Ber. Bunsen-Ges. Phys. Chem.* **1991**, *11*, 1376.
- (12) Inagaki, N.; Kondo, S.; Hirata, M.; Urushibata, H. *J. Appl. Polym. Sci.* **1985**, *30*, 3385.
- (13) Fonseca, J. L. C.; Badyal, J. P. S. *Macromolecules* **1992**, *25*, 4730.
- (14) Shard, A. G.; Munro, H. S.; Badyal, J. P. S. *Polym. Commun.* **1991**, *32*, 152.
- (15) Ehrlich, C. D.; Basford, J. A. *J. Vac. Sci. Technol.* **1992**, *A10*, 1.
- (16) Shard, A. G.; Badyal, J. P. S. *Macromolecules* **1992**, *25*, 2053.
- (17) Johansson, G.; Hedman, J.; Berndtsson, A.; Klasson, M.; Nilsson, R. *J. Electron Spectrosc.* **1973**, *2*, 295.
- (18) Graf, R. T.; Koekig, J. L.; Ishida, H. *Introduction to Optics and Infrared Spectroscopic Techniques. In Fourier Transform Infrared Characterization of Polymers*; Ishida, H., Ed.; Plenum Press: New York, 1987.
- (19) Hamada, K.; Morishita, H. *Spectrosc. Lett.* **1986**, *19*, 815.
- (20) Painter, P. C.; Coleman, M. M.; Koenig, J. J. *The Theory of Vibrational Spectroscopy and Its Application to Polymeric Materials*; Wiley: New York, 1982.
- (21) Inagaki, N.; Katsuoka, H. *J. Membr. Sci.* **1987**, *34*, 297.
- (22) Tajima, I.; Yamamoto, M. *J. Polym. Sci., Polym. Chem. Ed.* **1987**, *25*, 1737.
- (23) Cai, S.; Fang, J.; Xuehai, Yu. *J. Appl. Polym. Sci.* **1992**, *44*, 135.
- (24) Coopes, I. H.; Griesser, H. J. *J. Appl. Polym. Sci.* **1989**, *37*, 3413.
- (25) Wrobel, A. M.; Czeremuskin, G.; Szymanowski, H.; Kowalski, J. *Plasma Chem. Plasma Process.* **1990**, *10*, 277.
- (26) Apperley, D. C.; Harris, R. K.; Marshall, G. L.; Thompson, D. P. *J. Am. Ceram. Soc.* **1991**, *74*, 777.
- (27) Marsmann, H. *NMR* **1981**, *17*, 65.
- (28) Fonseca, J. L. C.; Apperley, D. C.; Badyal, J. P. S. *Chem. Mater.* **1992**, *4*, 1271.
- (29) Gambogi, R. J.; Cho, D. L.; Yasuda, H.; Blum, F. D. *J. Polym. Sci., Polym. Chem.* **1991**, *29*, 1801.
- (30) Kokai, F.; Kubota, T.; Ichijo, M.; Wakai, K. *Abstr. Pap.-Am. Chem. Soc.* **1987**, *193*, 117.
- (31) Pearse, R. W. B.; Gayon, A. G. *The Identification of Molecular Spectra*; Chapman and Hall: London, 1976.
- (32) Dike, G. H. In *The Hydrogen Molecule Wavelength Tables of G. H. Dieke*; Crosswhite, H. M., Ed.; Wiley-Interscience: New York, 1972.
- (33) Hollas, J. M. *Molecular Spectroscopy*; John Wiley & Sons: New York, 1987.
- (34) *Spectroscopic Data Relative to Diatomic Molecules*; Rosen, B., Ed.; Pergamon: Oxford, U.K., 1970.
- (35) Herzberg, G.; Phillips, J. G. *Astrophys. J.* **1948**, *163*, 108.
- (36) LeBlanc, F. J. *J. Chem. Phys.* **1968**, *48*, 1980.
- (37) Herzberg, H. *The Spectra and Structure of Simple Free Radicals*; Cornell University Press: Ithaca, NY, 1971.
- (38) Kiess, N. H.; Broida, H. P. *Astrophys. J.* **1956**, *123*, 166.
- (39) Moore, C. E.; Broida, H. P. *J. Res. Natl. Bur. Stand.* **1959**, *A-63*, 19.
- (40) Woo, S. C.; Liu, T. K.; Chu, T. C.; Chih, W. *J. Chem. Phys.* **1938**, *6*, 240.
- (41) Innes, K. K. *J. Chem. Phys.* **1954**, *22*, 863.

- (42) Ramsay, D. A.; Thistlewaite, P. *Can. J. Phys.* **1966**, *44*, 1381.
- (43) Woo, S. C.; Chu, T. C. *J. Chem. Phys.* **1937**, 786.
- (44) Yasuda, H. *Plasma Polymerization*; Academic Press: Orlando, FL, 1985.
- (45) Bell, A. T. *Fundamentals of Plasma Chemistry*; In *Techniques and Applications of Plasma Chemistry*; Hollahan, J. R., Bell, A. T., Eds.; John Wiley & Sons: New York, 1974.
- (46) Beidman, H.; Osada, Y. *Adv. Polym. Sci.* **1990**, *95*, 57.
- (47) Wolf, D. *Appl. Phys. Lett.* **1991**, *58*, 2081.
- (48) Morinaka, A.; Asano, Y. *J. Appl. Polym. Sci.* **1982**, *27*, 2139.
- (49) Thompson, L. F.; Smolinsky, G. *J. Appl. Polym. Sci.* **1972**, *16*, 1179.
- (50) Davidson, I. M. T.; Howard, A. V. *J. Chem. Soc., Faraday Trans.* **1975**, *71*, 69.
- (51) Pilcher, G.; Leita, M. L. P.; Meng-Yan, Y.; Walsh, R. *J. Chem. Soc. Faraday Trans. 1* **1991**, *841*, 249.
- (52) Cotton, F. A.; Wilkinson, G. *Advanced Inorganic Chemistry*; Wiley: New York, 1988.
- (53) Connor, B.; Finney, G. J.; Haszeldine, R. N.; Robinson, P. J.; Sedgwick, R. D.; Simmons, R. F. *J. Chem. Soc., Chem. Commun.* **1966**, 178.
- (54) Brix, T.; Bastian, E.; Potzinger, P. *J. Photochem. Photobiol. A* **1989**, *49*, 287.
- (55) Alexander, A. G.; Strausz, O. P. *J. Phys. Chem.* **1976**, *80*, 2531.
- (56) Ellul, R.; Potzinger, P.; Reimann, B. *J. Phys. Chem.* **1984**, *88*, 2793.
- (57) Wrobel, A. M.; Wertheimer, M. R. In *Plasma Deposition, Treatment, and Etching of Polymers*; d'Agostino, R., Ed.; Academic Press Inc.: San Diego, 1990; Chapter 3.

MA950222V